

# Rapid Kinetics of Protein–Nucleic Acid Interaction is a Major Component of HIV-1 Nucleocapsid Protein's Nucleic Acid Chaperone Function

Margareta Cruceanu<sup>1</sup>, Robert J. Gorelick<sup>2</sup>, Karin Musier-Forsyth<sup>3</sup>  
Ioulia Rouzina<sup>3\*</sup> and Mark C. Williams<sup>1,4\*</sup>

<sup>1</sup>Department of Physics  
Northeastern University  
111 Dana Research Ctr., Boston  
MA 02115, USA

<sup>2</sup>AIDS Vaccine Program  
SAIC-Frederick, Inc.  
NCI-Frederick, Frederick  
MD 21702, USA

<sup>3</sup>Department of Chemistry and  
Institute for Molecular Virology  
University of Minnesota  
207 Pleasant St. SE  
Minneapolis, MN 55455, USA

<sup>4</sup>Center for Interdisciplinary  
Research on Complex Systems  
Northeastern University  
111 Dana Research Ctr., Boston  
MA 02115, USA

The nucleic acid chaperone activity of the human immunodeficiency virus type-1 (HIV-1) nucleocapsid protein (NC) plays an important role in the retroviral life cycle, in part, by facilitating numerous nucleic acid rearrangements throughout the reverse transcription process. Recent studies have identified duplex destabilization and nucleic acid aggregation as the two major components of NC's chaperone activity. In order to better understand the contribution of the functional domains of NC to these two activities, we used optical tweezers to stretch single lambda DNA molecules through the helix-coil transition in the presence of wild-type or mutant HIV-1 NC. Protein-induced duplex destabilization was measured directly as an average decrease of the force-induced melting free energy, while NC's ability to facilitate strand annealing was determined by the amount of hysteresis in the DNA stretch-relax cycle. By studying zinc-free variants of full-length and truncated NC, the relative contributions of NC's zinc fingers and N-terminal basic domain to the two major components of chaperone activity were elucidated. In addition, examination of NC variants containing mutations affecting one or both zinc finger motifs showed that effective strand annealing activity is correlated with NC's ability to rapidly bind and dissociate from nucleic acids. NC variants with slow on/off rates are inefficient in strand annealing, even though they may still be capable of high affinity nucleic acid binding, duplex destabilization, and/or nucleic acid aggregation. Taken together, these observations establish the rapid kinetics of protein–nucleic acid interaction as another major component of NC's chaperone function.

© 2006 Elsevier Ltd. All rights reserved.

**Keywords:** nucleocapsid protein; nucleic acid chaperone; single molecule DNA stretching; DNA melting; DNA cooperativity

\*Corresponding authors

## Introduction

Human immunodeficiency virus type 1 (HIV-1) nucleocapsid protein (NC) participates in almost every step of the virus life cycle.<sup>1–3</sup> NC is only 55 amino acid residues (aa) long and is produced as a result of proteolytic processing of the Gag polyprotein,<sup>4</sup> which is the main player in virus

assembly.<sup>5</sup> In the context of Gag, NC functions as a nucleic acid binding domain, driving the self-assembly of Gag on nucleic acids.<sup>6–10</sup> Mature NC also functions as a nucleic acid chaperone, facilitating nucleic acid restructuring reactions that lead to more stable conformations.<sup>2,3,11–13</sup> In the absence of NC, these reactions are extremely slow because the original and intermediate nucleic acid structures are often very stable.<sup>14–17</sup> Based on numerous strand-exchange or annealing assays,<sup>13,14,18–21</sup> it has been suggested that the enhanced nucleic acid annealing or aggregating ability of NC, combined with its duplex destabilization activity, account for its chaperone activity.<sup>2,14,15</sup>

HIV-1 NC possesses two CCHC-type zinc finger motifs, which are flanked by largely unstructured

Abbreviations used: NC, nucleocapsid protein; aa, amino acid; ss, single-stranded; ds, double-stranded; HIV-1, human immunodeficiency virus type-1; FIM, force-induced melting; WT, wild-type.

E-mail addresses of the corresponding authors:  
rouzi002@umn.edu; mark@neu.edu

domains that contain multiple cationic residues (Figure 1). Upon nucleic acid binding, the 11 aa N-terminal domain of NC, which contains four basic residues, forms a  $3_{10}$  helix.<sup>22</sup> Removal of this domain greatly reduces NC's capability to induce nucleic acid aggregation.<sup>23–25</sup> The cationic nature of NC provides a major electrostatic contribution to its nucleic acid binding free energy, as shown by the strong salt dependence of NC–nucleic acid interactions.<sup>26,27</sup> NC will bind to both double-stranded (ds) and single-stranded (ss) nucleic acids, however, the zinc fingers preferentially interact with the latter. This interaction involves partial stacking of the aromatic residues Phe16 and Trp37 in the zinc finger domains with unpaired nucleic acid bases.<sup>22,28</sup> Although NC binding destabilizes structured nucleic acids,<sup>23,29,30</sup> it generally does not result in complete unwinding in the absence of a complementary strand.<sup>14,31–33</sup> Moreover, NC is a relatively weak destabilizing agent, with little or no effect on the stability of very stable nucleic acids.<sup>17,29,30,34</sup>

Single molecule DNA stretching, also referred to as force-induced melting (FIM), provides valuable information regarding the interaction between nucleic acids and proteins or small molecules that bind to ssDNA and dsDNA.<sup>35</sup> In these experiments, a single  $\lambda$ -DNA molecule is stretched to extensions that are almost twice its B-form contour length, resulting in a FIM transition. Extended regions of dsDNA melt cooperatively, and the midpoint of the melting transition,  $F_m$ , is analogous to the DNA melting temperature,  $T_m$ , obtained in thermal melting studies, and is similarly affected by solution conditions, such as pH, temperature, and ionic strength.<sup>36–38</sup> DNA binding proteins and small molecules that affect the thermal melting equilibrium of dsDNA have been shown to affect the FIM transition in a similar manner.<sup>37,39–46</sup> One advantage of the FIM method is that DNA melting studies are isothermal and can be performed over a wide range of temperatures, thus avoiding protein denaturation, and under solution conditions that allow the protein–DNA complex to aggregate.

The FIM technique may also reveal insights into the kinetics of protein–DNA interactions.<sup>40–42,47</sup> This is accomplished by measuring the pulling rate dependence of stretching curves, or by comparison of the force-extension profiles during DNA stretching and relaxation cycles in the absence and presence of protein. Analysis of the hysteresis, that is, the lack of an exact match between the stretch/

relax curves, reflects the ability of the strands to re-anneal. Therefore, performing stretch/relax cycles in the absence and presence of a DNA binding protein provides a quantitative measure of the protein's effect on nucleic acid strand annealing activity. In particular, when the DNA stretching and relaxation curves match, ssDNA created by stretching is able to anneal and form dsDNA on the time scale of relaxation, which is approximately 300 bp/s at a typical pulling (and relaxation) rate of 100 nm/s. This is the case in the absence of protein in high salt or in the presence of wild-type (WT) HIV-1 NC. However, when proteins bind to ssDNA but dissociate slowly from ssDNA on the time scale of the relaxation, annealing of the strands is slow, and this is reflected in large hysteresis observed during relaxation. This is the case in the presence of some of the zinc finger mutants studied here.

Here we employ single-molecule DNA stretching to probe NC's nucleic acid annealing, aggregation, and destabilization activities separately by examining mutants that are designed to be defective in one of these activities. Because the nucleic acid aggregating ability of NC is associated primarily with its cationic N-terminal tail,<sup>23–25,48</sup> while its duplex-destabilizing ability resides within the two zinc fingers,<sup>49,50</sup> we examined NC variants with changes to each of these regions. Thus, an N-terminal truncation mutant lacking the first ten aa (NC(11–55)), is expected to have diminished nucleic acid aggregating capabilities, while still maintaining duplex destabilizing activity, as previously shown.<sup>25,51</sup> In contrast, mutations that affect the zinc finger domains are expected to impact destabilization more than aggregation.

Surprisingly, our data show that DNA melted by force anneals efficiently even in the presence of high concentrations of NC variants known to be deficient in nucleic acid aggregation activity. We hypothesize that this effect is due to rapid protein dissociation from ssDNA. In addition, some NC proteins with mutations in the zinc finger domains, which should retain nucleic acid aggregation capabilities, strongly inhibit nucleic acid annealing, most likely due to slow protein dissociation. These results demonstrate that efficient nucleic acid annealing, an essential component of NC's chaperone activity, requires both nucleic acid aggregation and rapid nucleic acid binding and dissociation.

## Results

### Wild-type HIV-1 NC

#### *Equilibrium binding constant and effect on duplex stability*

The binding of saturating concentrations (30 nM or greater) of WT HIV-1 NC has a profound effect on both DNA stretching and relaxation curves (Figure 2(a) and (b)). The slope of the FIM transition increases dramatically, such that the transition

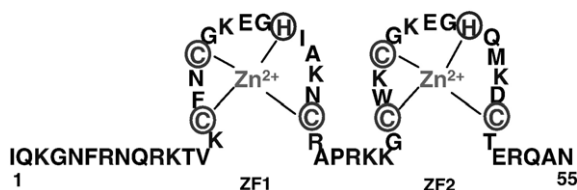


**Figure 1.** Amino acid sequence of HIV-1 NC (NL4-3 isolate). The zinc coordinating Cys and His residues are circled. ZF1 and ZF2 designate the two zinc finger motifs.

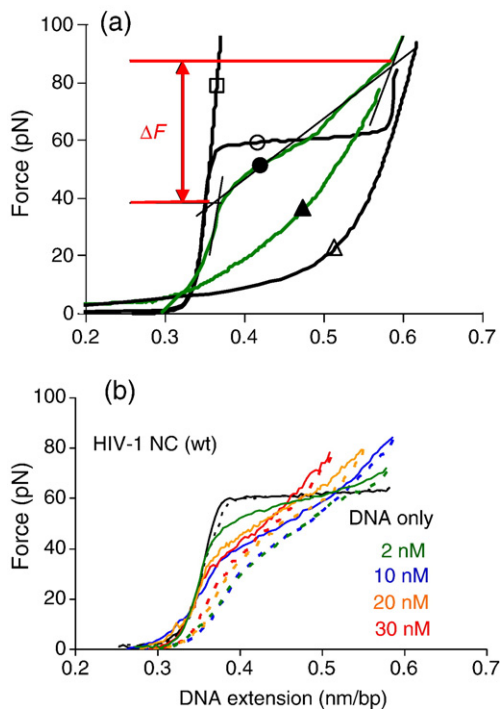


**Figure 2.** (a) Schematic illustration of the method used to determine  $\Delta F$ , the force transition width. Stretching curves for  $\lambda$ -DNA in the absence of protein (black curve, open circle), in the presence of 20 nM NCp7 (wild-type) protein (green curve, filled circle), and for ssDNA with NC bound on it (green curve, filled triangle), all in FIM buffer (see Materials and Methods) and at room temperature. For ssDNA with NC bound, data are from Williams *et al.*,<sup>36</sup> and were taken with 10 nM NCp7 in 25 mM NaCl, 10 mM Hepes (pH 7.5). Theoretical stretching curves for dsDNA (black curve, open square) and ssDNA (black curve, open triangle), fit to standard polymer models, in the absence of protein<sup>64</sup> are also shown. (b) DNA stretching (continuous lines) and relaxing (broken lines) curves in the absence and presence of WT HIV-1 NC. All measurements were performed in 50 mM Na<sup>+</sup> and protein concentrations are indicated.

takes place over a much broader force range than for DNA in the absence of protein (45 pN *versus* 3.5 pN, respectively). As discussed in previous work,<sup>47,52</sup> an equilibrium binding constant can be obtained by measuring the slope of the linear region of the force transition width,  $\Delta F$ , as a function of protein concentration,  $c$  (see equation (1) in Materials and Methods). The method of obtaining  $\Delta F$  is schematically illustrated in Figure 2(a). Using this method, a DNA association constant of  $1.22(\pm 0.24) \times 10^8 \text{ M}^{-1}$  was measured in 50 mM Na<sup>+</sup> (Table 1), in good agreement with bulk solution measurements.<sup>26,53–55</sup>

NC binding results in a significant decrease in the force required to stretch  $\lambda$ -DNA.<sup>47,49,50</sup> The free energy of dsDNA melting may be calculated from the area under a DNA stretch-relax cycle in which the dsDNA is stretched through its melting transition and released as ssDNA.<sup>46,47,49</sup> The DNA melting free energy,  $\Delta G_{\text{melt}}$ , in the presence of saturating concentrations of NC is 0.4 kcal/mol bp

**Table 1.** Binding parameters of WT and mutant HIV-1 NC

NC protein	$\Delta F_{\text{sat}}^a$ (pN)	$d(\Delta F)/dc^b$ (pN/nM)	$K_a^c$ ( $10^8 \text{ M}^{-1}$ )
No protein	$3.67 \pm 0.16$	–	–
wt NC	$44.7 \pm 1.9$	$5.02 \pm 0.97$	$1.22 \pm 0.24$
NC(11–55)	$41.7 \pm 2.0$	$0.45 \pm 0.10$	$0.12 \pm 0.01$
1-1	$51.0 \pm 2.2$	$3.25 \pm 0.06$	$0.69 \pm 0.03$
2-1	$30.0 \pm 1.3$	$0.77 \pm 0.06$	$0.32 \pm 0.05$
CCHH-CCHC	$29.7 \pm 1.4$	$2.40 \pm 0.06$	$0.92 \pm 0.05$
CCCC-CCHC	$8.1 \pm 0.34$	$0.15 \pm 0.06$	$0.33 \pm 0.13$

All data are based on the results shown in Figure 7 and are reported as averages  $\pm$  standard error for at least three experiments.

<sup>a</sup>  $\Delta F_{\text{sat}}$  is the maximum change in transition width observed in the presence of saturating protein concentrations.

<sup>b</sup>  $d(\Delta F)/dc$  is the slope of the linear portion of the curves shown in Figure 7.

<sup>c</sup>  $K_a$  is the apparent binding constant as determined from equation (1).

(a previously reported value of 0.8 kcal/mol bp was obtained at lower NC concentration),<sup>50</sup> which is about 1 kcal/mol bp smaller than in the absence of protein (Table 2). Thus, although NC significantly destabilizes the DNA duplex, it is unable to melt it completely.

### Non-equilibrium features of DNA stretching

In the presence of HIV-1 NC, the DNA relaxation curves are quite regular, and very similar in shape to the stretching curves (Figure 2(b)). The extent of hysteresis observed in the stretch-relax curves depends on the amount of NC bound. As shown in Figure 2(b), at low NC concentrations, the hysteresis is significantly larger than that observed in the absence of protein. The hysteresis is once again reduced upon reaching saturating levels of

**Table 2.** Parameters describing DNA melting

NC protein	Conc <sup>a</sup> (nM)	$\Delta G_{\text{melt}}^b$ (kcal/mol bp)	$\delta G_{\text{net}}^c$ (kcal/mol bp)	$\Delta G_{\text{hysteresis}}^d$ (kcal/mol bp)
No protein		$1.51 \pm 0.08$	–	$0.22 \pm 0.06$
wt NC	20	$0.44 \pm 0.05$	1.1	$0.22 \pm 0.06$
NC(11–55)	100	$1.22 \pm 0.50$	0.3	$0.25 \pm 0.06$
1-1	20	$0.67 \pm 0.10$	0.84	$0.24 \pm 0.10$
2-1	100	$0.58 \pm 0.14$	0.93	$0.48 \pm 0.09$
CCHH-CCHC	7	$0.83 \pm 0.10$	0.68	$0.67 \pm 0.03$
CCCC-CCHC	100	$0.85 \pm 0.16$	0.66	$0.37 \pm 0.10$
NC+EDTA <sup>e</sup>	5	$1.65 \pm 0.05$	–0.14	$0.62 \pm 0.04$
SSHS-SSHS	10	$1.75 \pm 0.16$	–0.24	$0.42 \pm 0.10$

<sup>a</sup> All measurements were performed at concentrations close to saturation. Data are reported as averages  $\pm$  standard error for at least three experiments.

<sup>b</sup>  $\Delta G_{\text{melt}}$  is the melting free energy per base-pair obtained from the area between dsDNA and ssDNA stretching curves.

<sup>c</sup>  $\delta G_{\text{net}}$  is the net duplex destabilization, i.e.  $\Delta G_{\text{melt}}$  (no protein) –  $\Delta G_{\text{melt}}$  (with protein).

<sup>d</sup>  $\Delta G_{\text{hysteresis}}$  is the area between stretching and relaxing curves. It represents the free energy per base-pair lost during the stretch-relax cycle.

<sup>e</sup> NC+EDTA was obtained by adding 1 mM EDTA in the FIM buffer (see Materials and Methods). Control experiments using the same buffer did not show any effect of EDTA on DNA stretch-relax curves.

NC ( $\geq 10$  nM). Our interpretation of these observations is that at sub-saturating binding, NC does not induce strand attraction, and instead makes the strands bulkier and less mobile due to hydrodynamic friction, thus slowing down their annealing. This conclusion is in accord with the fact that multivalent cation-induced nucleic acid attraction requires saturating amounts of bound cations.<sup>56</sup>

### Zinc-free NC

To examine the role of the zinc fingers in duplex destabilization and strand re-annealing, DNA stretching studies were carried out with two zinc-free forms of NC. SSHS-SSHS NC is a variant in which all cysteine residues have been substituted with serine. Although this variant was previously analyzed by DNA stretching,<sup>49</sup> this earlier work focused on the protein's inability to destabilize DNA, and did not quantitatively examine its overall effects on nucleic acid stability. A second zinc-free variant was obtained by EDTA-treatment.<sup>18</sup> Here, we will use these proteins to quantify and dissect the binding component responsible for cationic stabilization of nucleic acids from the overall destabilizing effect of WT NC.

The DNA stretching curves obtained with zinc-free NC proteins are presented in Figure 3. In both cases, the shape of the curves differed significantly from the curves obtained with WT NC (Figure 2(b)), and was similar to the curves obtained in the absence of protein, except for a small difference in the initial stretching force, which is likely due to nucleic acid attraction induced by the presence of the cationic NC protein. Based on this and previous analyses,<sup>49,50,47</sup> we conclude that the zinc fingers are responsible for NC's duplex-destabilizing activity.

The melting force,  $F_{mv}$ , was 1–6 pN higher in the presence of SSHS-SSHS NC or NC+ EDTA relative to free DNA (Figure 3), and similar to that measured for  $\lambda$ -DNA in high salt.<sup>38</sup> Assuming that both the ds and ss DNA elasticity are the same in the presence of mutant NC as in the absence of protein (a reasonable assumption given the negligible change in shape of the melting transition), the free energy of dsDNA

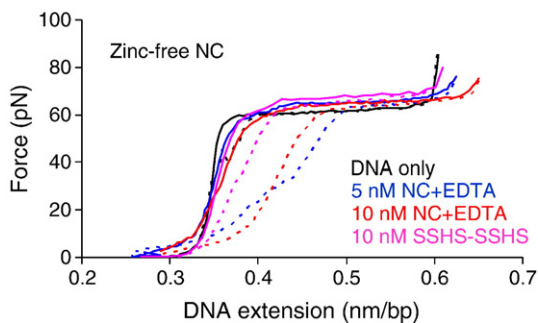


**Figure 3.** DNA stretching (continuous lines) and relaxing (broken lines) curves in the absence and presence of zinc-free variants of HIV-1 NC. All measurements were performed in 50 mM Na<sup>+</sup> and proteins used and their concentrations are indicated.

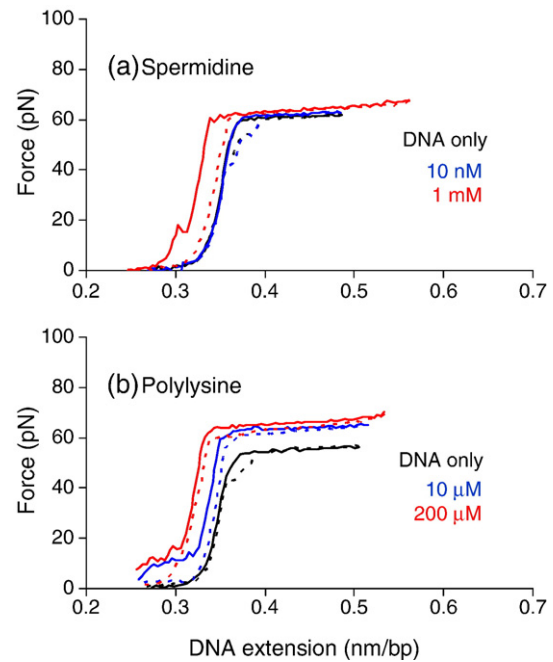


**Figure 4.** DNA stretching (continuous lines) and relaxing (broken lines) curves in the absence and presence of spermidine in 50 mM Na<sup>+</sup> (a) and polylysine in 6.2 mM Na<sup>+</sup> (b).

melting per base-pair is calculated to be 1.75 kcal/mol bp and 1.65 kcal/mol bp for 10 nM SSHS-SSHS NC and 5 nM NC+ EDTA, respectively (Table 2). These values are slightly higher than that observed for  $\lambda$ -DNA in the absence of protein (Table 2). The average stabilization of DNA,  $-\delta G_{net}$ , by the two forms of zinc-free NC is  $\sim 0.2$  kcal/mol bp (Table 2). If we assume that this electrostatic stabilization is of similar magnitude for WT NC, and given that the net destabilization of duplex DNA due to WT NC is 1.1 kcal/mol bp ( $\delta G_{net}$ , Table 2), the overall contribution of NC's zinc fingers to DNA destabilization is given by:  $\delta G^{ZF} = \delta G^{NC} - \delta G^{el} = 1.1 - (-0.2) = 1.3$  kcal/mol bp.

The DNA stretch-relax curves in the presence of SSHS-SSHS NC display modest levels of hysteresis, suggesting that SSHS-SSHS NC is fairly effective at promoting strand annealing. In addition, the contour length of dsDNA in subsequent stretches of the same DNA molecule does not change (data not shown). This is an indication that, similar to WT NC, SSHS-SSHS NC is a “fast” protein that rapidly dissociates from ssDNA and readily rebinds dsDNA upon relaxation. The NC+EDTA curves show greater hysteresis, but about half of the relaxation curve exactly matches the stretching curve. This suggests that much of the NC+EDTA rapidly dissociates from ssDNA, but that some portions remain bound and inhibit re-annealing.

### Comparison with simple multivalent cations

Figure 4 shows typical DNA stretch-relax curves obtained in the presence of a small trivalent

polyamine, spermidine (a), and in the presence of poly-D-lysine (b). The primary interaction between these simple multivalent cations and nucleic acids is electrostatic, and these cations are known to maintain their hydration shell and remain highly mobile when bound to nucleic acids.<sup>56</sup> Due to the higher phosphate charge density, binding is slightly stronger to dsDNA relative to ssDNA,<sup>57–59</sup> resulting in slight stabilization of duplexes. This is consistent with the observed increase in the  $F_m$  (Figure 4). With the exception of the overall increase in  $F_m$ , the shape of the stretching curve remains unchanged relative to that observed in the absence of ligand. The duplex stabilization induced by these cations is similar to what was observed in the presence of zinc-free NC. In addition, the DNA relaxation curves show negligible hysteresis in the DNA melting plateau region. There is some hysteresis at extensions less than 0.34 nm/bp, but this is due to DNA condensation and aggregation, and does not reflect any inhibition of re-annealing. Due to interference from this aggregation effect, we did not perform a full titration of the cations to saturating concentrations. However, all of the data obtained are consistent with the hypothesis that DNA strand annealing in the presence of these simple cations is extremely fast, which suggests that these ligands are capable of very fast ds and ss DNA binding and dissociation, and that they effectively promote strand annealing by inducing attraction between DNA strands. Here “extremely fast” means faster than the time required for stretching and relaxation. While we cannot determine precisely how fast this is, the absence of hysteresis in our relaxation curves means that the base-pairs anneal faster than  $10^4$  bp/s. In the absence of protein the re-annealing rate from the helix/coil boundary is  $\sim 10^7$  bp/s. This gives the possible range of annealing rates in our experiments.

### N-terminal truncation mutant

We next stretched single DNA molecules in the presence of NC(11–55), a deletion mutant that lacks the first ten residues. It is well-established that the N-terminal cationic domain is a major factor in NC's nucleic acid binding and aggregation activity.<sup>23–26</sup> Indeed, much higher concentrations of NC(11–55) relative to WT NC are required to produce significant changes to the DNA stretching curves (Figure 5). The measured binding affinity of  $K_a = 0.12(\pm 0.01) \times 10^8 \text{ M}^{-1}$  in 50 mM NaCl, is  $\sim$ ten times lower than that of WT NC (Table 1). This measurement agrees well with bulk solution measurements of NC(11–55),<sup>27</sup> NC(12–55),<sup>48,60</sup> and NC(12–53)<sup>26</sup> binding to various nucleic acid substrates.

At saturating protein concentrations ( $>100$  nM), the shape of the DNA stretching curve resembles that of WT NC. The saturated force transition width is also similar to WT NC ( $\sim 40$  pN), but is reached at  $\sim 20$ -fold higher protein concentrations, i.e. 200 nM. The  $F_m$  however, is  $\sim 10$  pN higher than that observed in the presence of saturating concentrations of WT NC. Therefore, at saturation, NC(11–55)

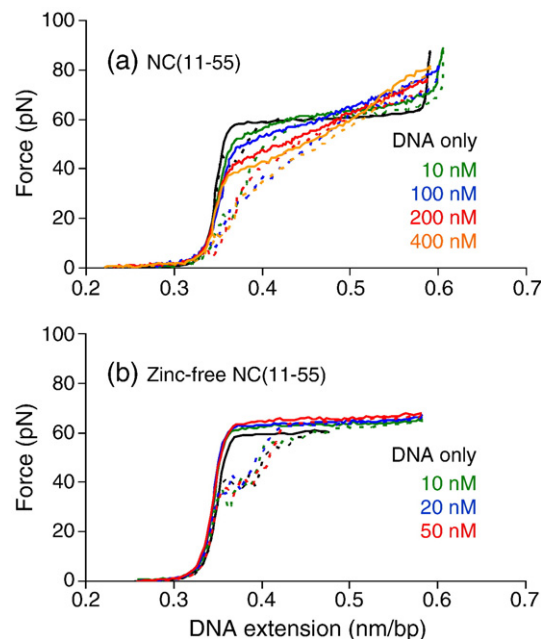


**Figure 5.** DNA stretching (continuous lines) and relaxing (broken lines) curves obtained in the absence and presence of NC(11–55) (a) and EDTA-treated zinc-free NC(11–55) (b).

destabilizes the DNA duplex by only  $\sim 0.3$  kcal/mol bp, as compared to  $\sim 1.1$  kcal/mol bp for WT NC (Table 2).

Most notably, the DNA relaxation curves in the presence of NC(11–55) do not retain the same shape as the stretching curves. However, the total amount of hysteresis,  $\Delta G_{\text{hysteresis}} \sim 0.25$  kcal/mol bp (Table 2), is similar to that observed in the absence of protein or in the presence of WT NC. The overall shape of the hysteresis with NC(11–55) is similar to that observed in the presence of low concentrations of WT NC. Because it is only at high protein concentrations that WT NC's strand annealing is enhanced due to nucleic acid aggregation, this result is consistent with a role of the N-terminal domain in NC's aggregation capability. In repeated stretch-relax cycles of the same DNA molecule, the dsDNA contour length is highly reproducible (data not shown), suggesting that NC(11–55) can rapidly dissociate from ssDNA and rebind dsDNA in a manner that does not interfere with strand re-annealing. Taken together, these findings suggest that NC(11–55) lacks electrostatic strand attraction capabilities, but does not prevent DNA re-annealing in single molecule stretching experiments, where the two strands are held in close proximity. In contrast, NC(11–55) is not efficient at nucleic acid aggregation or strand annealing in bulk solution studies, where electrostatic strand attraction is required.<sup>24,25,65</sup>

The stretching and relaxation curves in the presence of zinc-free NC(11–55) generated by treatment with EDTA are very similar to those obtained in the absence of protein (Figure 5(b)). This shows that both duplex destabilizing and strand annealing activities of NC are suppressed by simultaneously

eliminating the N-terminal cationic domain and the zinc finger structures.

### HIV-1 NC zinc finger mutants

All NC zinc finger mutants used here retain their cationic and aromatic residues. Thus, the effect of these mutations on nucleic acid aggregation should be minimal. In the 1-1 mutant, the first zinc finger is duplicated, whereas in 2-1 NC, the two native zinc fingers are interchanged. We also tested two mutants with a non-native N-terminal zinc finger, CCHH-CCHC NC and CCCC-CCHC NC. Although previous stretching studies were performed with these variants,<sup>49,50</sup> a more extensive analysis is reported here, wherein we quantify the effect of these mutations on NC's duplex destabilization activity and melting force transition width. In addition, the effects of these mutations on the protein-DNA interaction kinetics are examined for the first time.

#### 1-1 mutant

The DNA stretch-relax curves in the presence of 1-1 NC are similar to those obtained with WT NC (Figure 6(a)). The association constant of 1-1 NC to ssDNA is  $0.69(\pm 0.03) \times 10^8 \text{ M}^{-1}$ , which is less than twofold weaker than WT NC. The saturated force transition width is  $\sim 51 \text{ pN}$ , and the net duplex destabilization is  $\sim 0.8 \text{ kcal/mol bp}$  (Tables 1 and 2). These values reflect somewhat weaker preferential binding of the mutant to ssDNA, which should lead to less duplex destabilization activity. The relaxation curves in the presence of 1-1 NC are similar in shape to the relaxation curves with WT NC. The hysteresis is very small and decreases at higher protein concentrations. At the end of each stretch-relax cycle, the protein readily dissociates from ssDNA and rebinds to the annealed dsDNA. These features suggest that 1-1 NC is as efficient in promoting DNA strand annealing as the WT protein, and is only a slightly weaker duplex destabilizer.

#### 2-1 mutant

The 2-1 mutant has a reduced binding constant relative to WT NC, with  $K_a = 0.32(\pm 0.05) \times 10^8 \text{ M}^{-1}$  (Table 1). Its effect on the DNA melting transition width saturates at a relatively small value, with  $\Delta F_{\text{sat}} \sim 30 \text{ pN}$  (Figure 7 and Table 1). The estimated duplex destabilization induced by 2-1 NC,  $\Delta G_{\text{net}} \sim 0.93 \text{ kcal/mol}$  is significant, but smaller than that induced by WT NC (Table 2). However, this protein produces DNA melting hysteresis that is twice that observed in the absence of protein or in the presence of WT NC or the 1-1 mutant (Figure 6(c) and Table 2). In contrast to WT NC, the amount of hysteresis increases with 2-1 NC concentration. Moreover, in some cases, subsequent stretches of the same molecule showed a longer apparent dsDNA contour length, suggesting that the relaxed DNA retains partial single-stranded character (Figure 6(c)). These observations suggest

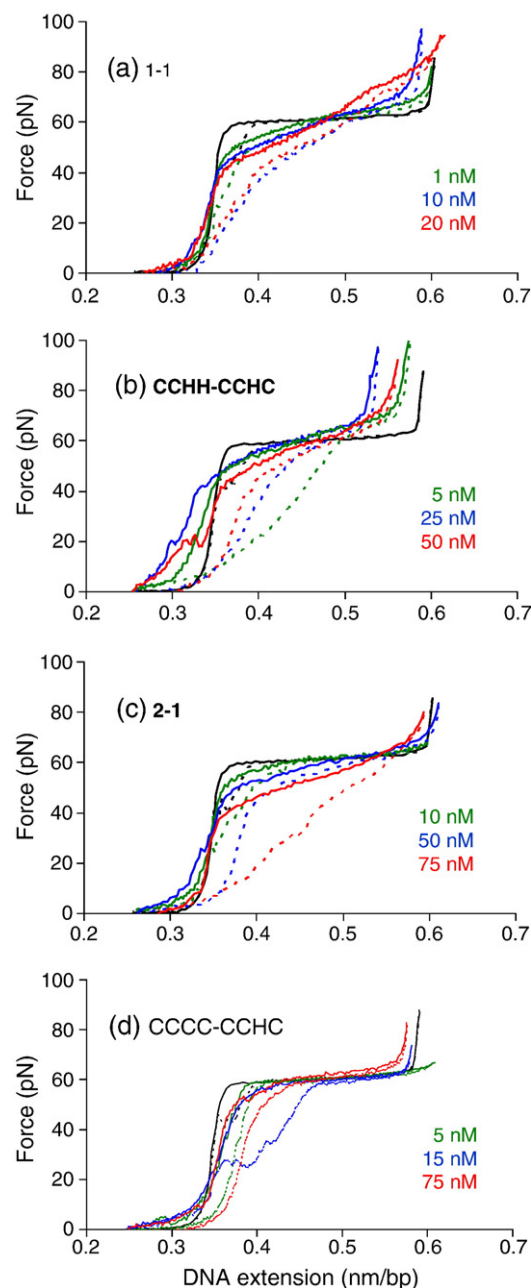


**Figure 6.** DNA stretching (continuous lines) and relaxing (broken lines) curves in the absence and presence of zinc finger mutants: 1-1 NC (a); CCHH-CCHC NC (b); 2-1 NC (c); CCCC-CCHC NC (d). Protein concentrations are indicated.

that, while the 2-1 mutant is a good duplex destabilizer, it is relatively slow to dissociate from ssDNA, and therefore interferes significantly with DNA strand annealing.

#### CCHH-CCHC mutant

The CCHH-CCHC NC mutant has a ssDNA association constant that is only slightly smaller than that of WT NC,  $K_a = 0.92(\pm 0.05) \times 10^8 \text{ M}^{-1}$  (Table 1), in good agreement with other binding

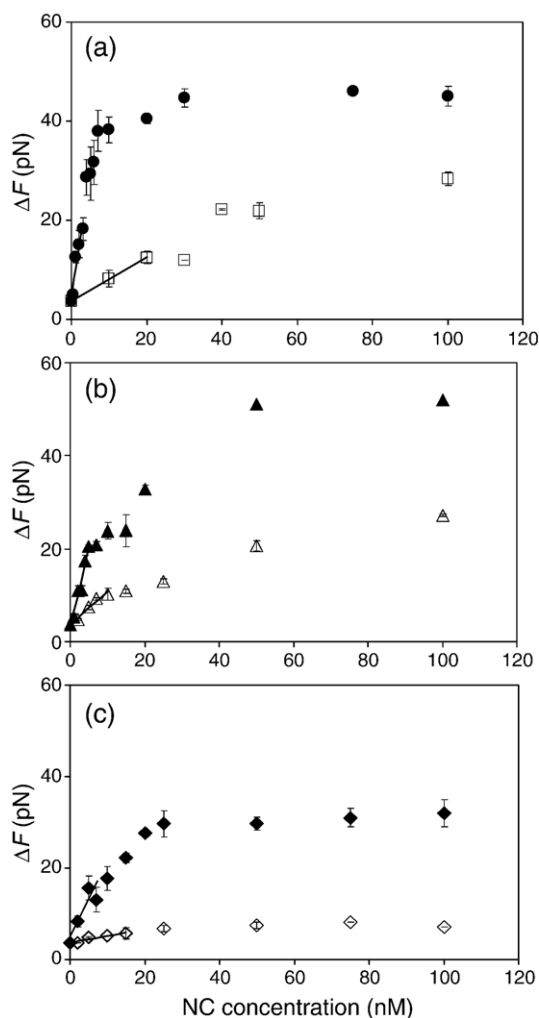


**Figure 7.** Titration curves for WT and mutant HIV-1 NC binding to single  $\lambda$ -DNA molecules: (a) WT NC (●) and (11-55)NC (□); (b) 1-1 NC (▲) and 2-1 NC (△); (c) CCHH-CCHC NC (◆) and CCCC-CCHC NC (◇). The lines represent the linear fits in the low concentration region.

studies.<sup>27</sup> The effect of saturating CCHH-CCHC NC on the DNA melting transition width is reduced ( $\sim 30$  pN, Figure 7), which suggests that this mutant has weaker duplex destabilization activity than WT NC. Consistent with this conclusion, the net duplex destabilization measured for this variant is  $\Delta G_{\text{melt}} \sim 0.7$  kcal/mol, which is significantly lower than that observed in the presence of WT NC. The DNA relaxation curves are quite regular and similar in shape to the stretching curves. However, this mutant produces significantly more hysteresis than WT NC, by about a factor of 3, which is even greater than that produced by 2-1 NC (Figure 6(b)). In addition, the apparent dsDNA contour length appears significantly shorter than that observed in the absence of protein, and varies greatly between stretch-relax cycles of the same molecule, suggesting a slow off rate. Thus, although its binding affinity to DNA is comparable to that of WT NC, this mutant is defective in both duplex destabilization and strand annealing.

#### CCCC-CCHC mutant

The CCCC-CCHC NC mutant binds to ssDNA with  $\sim$ fourfold lower affinity than WT NC, with  $K_a = 0.33(\pm 0.13) \times 10^8 \text{ M}^{-1}$  (Table 1). Its effect on the shape of the DNA stretching curves is minor even at saturation, with  $\Delta F_{\text{sat}} \sim 8$  pN (Table 1). The DNA melting transition remains flat and its midpoint is slightly increased compared to that observed in the absence of protein (Figure 6(d)), suggesting no duplex destabilizing activity for this mutant. Also, DNA stretch-relax cycles with CCCC-CCHC NC are characterized by modest hysteresis, with  $\Delta G_{\text{hysteresis}} \sim 0.4$  kcal/mol bp (Table 2). The shapes of the DNA extension and relaxation curves are also quite similar. These features are very similar to those obtained with the zinc-free NC, and suggest that this mutant has the properties of a cationic ligand, which efficiently promotes strand annealing, but which may have severe defects in chaperone activity due to its inability to destabilize duplex structures.

## Discussion

Here, single molecule  $\lambda$ -DNA stretching studies were used to characterize the thermodynamics and kinetics of NC's interaction with nucleic acids. All of the measured parameters are averaged over the 48,500 bp length of polymeric  $\lambda$ -DNA. Thus, here, we gain insights into the properties of HIV-1 NC that contribute to its sequence-non-specific nucleic acid interactions rather than to sequence-specific binding properties.

In accord with previous studies, reviewed by Levin *et al.*,<sup>2</sup> we find that two major properties of NC contribute to its chaperone function: (i) moderate base-pair destabilization activity, and (ii) nucleic acid strand annealing activity. In particular, we find that polymeric duplex DNA remains quite stable in the presence of saturating concentrations of NC, with an average base-pair stability of  $\sim 0.4$  kcal/mol bp and a net duplex destabilization of 1.1 kcal/mol bp in 50 mM  $\text{Na}^+$ . In contrast to these results obtained with long duplex DNA strands, short nucleic acid helices are significantly destabilized by NC.<sup>14-17,29,30,33,34,48,60,61</sup> This effect is most likely due to the fact that the destabilizing free energy of helix boundaries has a much greater relative effect on the stability of short helices compared to that of long helices. NC's moderate duplex destabilizing ability is a key feature of its chaperone function because it helps nucleic acids to escape kinetic folding traps but does not destabilize the final maximally base-paired state.

This study is consistent with previous work<sup>20,21,49,50</sup> showing that, in general, mutations in NC's zinc finger structures result in significantly weaker NC-induced duplex destabilization, even at saturated protein binding, and illustrates the importance of the specific conformation and relative positioning of the two zinc fingers. Zinc-free NC produced

moderate duplex stabilization, similar to the effects of multivalent cations. In all cases, the stabilizing effects are the result of effective charge screening of DNA phosphates by polycationic species.<sup>57,59</sup>

The protein-DNA binding constants measured here for WT and mutant NCs correspond to sequence-non-specific binding to ssDNA. WT NC demonstrated the strongest binding, while the NC (11–55) mutant lacking the cationic N-terminal domain bound ~tenfold more weakly than WT NC. Thus, electrostatic interactions constitute a major component of NC's nucleic acid binding activity. Of all the zinc finger variants examined, the largest decreases in binding affinity were observed for 2-1 NC and CCCC-CCHC NC (~four-fold). This small variation in binding strength is unlikely to be significant *in vivo*, as the NC concentration in the virion (estimated to be >1 mM) significantly exceeds the protein's dissociation constant.

A major component of NC's nucleic acid chaperone function is its ability to promote the bimolecular association step of nucleic acid annealing reactions. This activity was previously believed to be associated exclusively with NC's ability to promote nucleic acid aggregation.<sup>2</sup> This study extends our understanding of NC's ability to promote strand annealing by examining the amount of hysteresis observed in the DNA stretch-relax cycles. Large hysteresis reflects slower strand annealing, despite the fact that the two DNA strands are held in close proximity in these experiments. Thus, the amount of hysteresis observed in the presence of different NC variants is a quantitative measure of the protein's strand annealing ability. According to this study, the amount of hysteresis (in terms of the average free energy lost per base-pair in a stretch-relax cycle, see Table 2) increases in the order: spermidine and polylysine < WT NC < 1-1 < NC(11–55) < CCCC-CCHC < SSHS-SSHS < 2-1 < NC+EDTA < CHH-CCHC. Note that while quantitative hysteresis results for spermidine and polylysine are not presented in Table 2, all of the stretching curves showed negligible hysteresis in the presence of these cations in the melting plateau region. For most of these proteins, except for NC(11–55), 2-1 and CHH-CCHC, hysteresis decreased with increasing protein concentration, indicating that strand annealing was actively promoted only in the presence of saturating concentrations of protein.

The rapid kinetics of a protein-DNA interaction is indicated by DNA extension curves that are highly reproducible at various pulling rates and in repeated cycles. These characteristics are indicative of an equilibrium process, which in the presence of a DNA binding protein implies its rapid adjustment to changes in the DNA secondary structure. In general, one would expect that highly charged molecules such as WT NC, specific zinc finger mutants, and the multivalent cations examined here, should be very efficient at strand annealing due to induced electrostatic attraction. This is indeed the case for WT NC,

multivalent cations, and 1-1 NC. However, the rest of the zinc finger mutants showed significant hysteresis, suggesting that the zinc finger mutations reduce NC's strand annealing capabilities. Based on these data, we conclude that nucleic acid aggregation is necessary but not sufficient for effective annealing activity. Rapid kinetics of protein-nucleic acid interaction is also an important component of chaperone function. Of all the NC mutants studied here, only the 1-1 mutant retains both annealing capabilities (aggregation and rapid binding kinetics), along with effective duplex destabilization activity. These results are in accord with previous *in vitro* minus-strand transfer annealing assays.<sup>20</sup>

Interestingly, the amount of hysteresis observed with NC(11–55) was relatively small, while stretching and relaxation curves were reproducible and pulling rate independent (Figure 5(a) and Table 2). However, the shape of the stretching and relaxation curves remained quite different even at saturated NC(11–55) binding, suggesting the absence of protein-induced strand attraction, as expected for this variant. We hypothesize that the small amount of hysteresis observed is not due to protein-promoted strand annealing, but is due to this variant's ability to rapidly adjust to the state of DNA (i.e. ss *versus* ds) as the two strands anneal.

The two functions of NC as a nucleic acid chaperone, its duplex destabilizing and nucleic acid strand annealing activities, oppose each other. Indeed, the first activity relies on the ability of NC to bind preferentially to ss nucleic acids. In contrast, strand annealing activity relies mainly on the simple cationic properties of NC, leading to delocalized nucleic acid binding. However, high mobility of a nucleic acid binding protein is incompatible with more specific primarily hydrophobic interactions that make single-stranded DNA a preferred substrate for NC binding. This study suggests that HIV-1 NC protein optimizes its nucleic acid chaperone properties by compromising both activities. Thus, it is a weak duplex destabilizer and a cationic protein with less than optimal (relative to small multivalent cations) strand annealing ability.

In summary, we have shown here that, while simple cationic attraction is an important component of nucleic acid chaperone activity, an additional requirement is the ability of the protein to rapidly adjust to ss and ds DNA binding states. Thus, while all of the zinc finger mutants examined retain the same high charge density and should therefore electrostatically facilitate strand annealing, the specific changes in nucleic acid binding induced by these mutations alter both duplex destabilization and protein binding kinetics. In all cases, either the protein's strand annealing capability or its duplex destabilization is compromised by mutation. Additional studies are needed to determine why NC's specific zinc finger structure is the optimum structure to facilitate such rapid protein binding kinetics.

## Materials and Methods

The optical tweezers instrument and data acquisition were as described.<sup>49,50</sup> Biotinylated lambda DNA was prepared and captured as described.<sup>62</sup> The DNA was labeled at the 3'-ends such that it would be free to rotate when stretched. WT and mutant HIV-1 NC proteins, were prepared as described.<sup>20,63</sup> Proteins were stored at -80 °C in 10 µl aliquots at 10, 25 or 50 µM protein concentration in NC-storage buffer (20 mM Hepes, 5 mM β-mercaptoethanol, 0.1 mM Tris (2-carboxyethyl)phosphine hydrochloride, pH 7.5). The buffer used for most of the FIM experiments (FIM buffer) contained 50 mM Na<sup>+</sup> (10 mM Hepes, 45 mM NaCl, 5 mM NaOH, pH 7.5). DNA stretch-relax cycles with polylysine were also performed in 6.2 mM Na<sup>+</sup> buffer (10 mM Hepes, 1.2 mM NaCl, 5 mM NaOH, pH 7.5). To obtain the zinc-free variants of WT and NC(11-55), 1 mM EDTA was added to the FIM buffer and 1 µM NC or NC(11-55) was incubated in this buffer for at least 10 min before use. Spermidine and polylysine were purchased from Sigma and were dissolved in de-ionized water before use.

The equilibrium binding constant was calculated using the following equation:

$$K_a = \frac{1}{\delta F_{\text{sat}}} \cdot \frac{\delta F(c)}{c} = \frac{1}{\delta F_{\text{sat}}} \cdot \left. \frac{d(\delta F(c))}{dc} \right|_{c \rightarrow 0} \quad (1)$$

where  $\delta F(c) = \Delta F^{\text{NC}} - \Delta F^{\text{no protein}}$  is the change in the transition width due to the addition of NC at the concentration  $c$ ,  $\delta F_{\text{sat}}$  is  $\delta F$  at saturating protein binding, and  $d(\delta F(c))/dc$  is the slope of  $\delta F(c)$  versus  $c$  in the low concentration (linear) region. The transition width was determined as shown in Figure 2(a).

## Acknowledgements

This project has been funded in whole or in part with federal funds from the National Cancer Institute, National Institutes of Health, under contract N01-CO-12400 (R.J.G.). The content of this publication does not necessarily reflect the views or policies of the Department of Health and Human Services, nor does mention of trade names, commercial products, or organizations imply endorsement by the U.S. Government. This work was also funded by the National Science Foundation (MCB-0238190), the National Institutes of Health (GM072462 to M.C.W. and GM065056 to K.M.-F.), and the Research Corporation.

## References

- Darlix, J.-L., Lapadat-Tapolsky, M., de Rocquigny, H. & Roques, B. P. (1995). First glimpses at structure-function relationships of the nucleocapsid protein of retroviruses. *J. Mol. Biol.* **254**, 523–537.
- Levin, J. G., Guo, J., Rouzina, I. & Musier-Forsyth, K. (2005). Nucleic acid chaperone activity of HIV-1 nucleocapsid protein: critical role in reverse transcription and molecular mechanism. In *Progress in Nucleic Acid Research and Molecular Biology* (Elsevier, ed), vol. 80, pp. 217–286. Academic Press.
- Rein, A., Henderson, L. E. & Levin, J. G. (1998). Nucleic-acid-chaperone activity of retroviral nucleocapsid proteins: significance for viral replication. *Trends Biochem. Sci.* **23**, 297–301.
- Henderson, L. E., Bowers, M. A., Sowder, R. C., 2nd, Serabyn, S. A., Johnson, D. G., Bess, J. W., Jr *et al.* (1992). Gag proteins of the highly replicative MN strain of human immunodeficiency virus type 1: posttranslational modifications, proteolytic processings, and complete amino acid sequences. *J. Virol.* **66**, 1856–1865.
- Swanstrom, R. & Wills, J. (1997). Synthesis, assembly, and processing of viral proteins. In *Retroviruses* (Coffin, J. M., Hughes, S. H. & Varmus, H., eds), pp. 263–334. Cold Spring Harbor Laboratory Press, Cold Spring Harbor, NY.
- Vogt, V. M. (1987). Retroviral virions and genomes. In *Retroviruses* (Coffin, J. M., Hughes, S. H. & Varmus, H. E., eds), pp. 27–70. Cold Spring Harbor Laboratory Press, Cold Spring Harbor, NY.
- Campbell, S. & Vogt, V. M. (1995). Self-assembly in vitro of purified CA-NC proteins from Rous sarcoma virus and human immunodeficiency virus type 1. *J. Virol.* **69**, 6487–6497.
- Campbell, S. & Rein, A. (1999). In vitro assembly properties of human immunodeficiency virus type 1 Gag protein lacking the p6 domain. *J. Virol.* **73**, 2270–2279.
- Campbell, S., Fisher, R. J., Towler, E. M., Fox, S., Issaq, H. J., Wolfe, T. *et al.* (2001). Modulation of HIV-like particle assembly in vitro by inositol phosphates. *Proc. Natl Acad. Sci. USA*, **98**, 10875–10879.
- Muriaux, D., Mirro, J., Harvin, D. & Rein, A. (2001). RNA is a structural element in retrovirus particles. *Proc. Natl Acad. Sci. USA*, **98**, 5246–5251.
- Herschlag, D. (1995). RNA chaperones and the RNA folding problem. *J. Biol. Chem.* **270**, 20871–20874.
- Lorsch, J. R. (2002). RNA chaperones exist and DEAD box proteins get a life. *Cell*, **109**, 797–800.
- Tsuchihashi, Z. & Brown, P. O. (1994). DNA strand exchange and selective DNA annealing promoted by the human immunodeficiency virus type 1 nucleocapsid protein. *J. Virol.* **68**, 5863–5870.
- Hargittai, M. R. S., Gorelick, R. J., Rouzina, I. & Musier-Forsyth, K. (2004). Mechanistic insights into the kinetics of HIV-1 nucleocapsid protein-facilitated tRNA annealing to the primer binding site. *J. Mol. Biol.* **337**, 951–968.
- DeStefano, J. J. (1996). Interaction of human immunodeficiency virus nucleocapsid protein with a structure mimicking a replication intermediate. Effects on stability, reverse transcriptase binding, and strand transfer. *J. Biol. Chem.* **271**, 16350–16356.
- Driscoll, M. D. & Hughes, S. H. (2000). Human immunodeficiency virus type 1 nucleocapsid protein can prevent self-priming of minus-strand strong stop DNA by promoting the annealing of short oligonucleotides to hairpin sequences. *J. Virol.* **74**, 8785–8792.
- Heilman-Miller, S., Wu, T. & Levin, J. G. (2004). Alteration of nucleic acid structure and stability modulates the efficiency of minus-strand transfer mediated by the HIV-1 nucleocapsid protein. *J. Biol. Chem.* **279**, 44154–44165.
- Dib-Hajj, F., Khan, R. & Giedroc, D. P. (1993). Retroviral nucleocapsid proteins possess potent nucleic acid strand renaturation activity. *Protein Sci.* **2**, 231–243.

19. You, J. C. & McHenry, C. S. (1994). Human immunodeficiency virus nucleocapsid protein accelerates strand transfer of the terminally redundant sequences involved in reverse transcription. *J. Biol. Chem.* **269**, 31491–31495.
20. Guo, J., Wu, T., Kane, B. F., Johnson, D. G., Henderson, L. E., Gorelick, R. J. & Levin, J. G. (2002). Subtle alterations of the native zinc finger structures have dramatic effects on the nucleic acid chaperone activity of human immunodeficiency virus type 1 nucleocapsid protein. *J. Virol.* **76**, 4370–4378.
21. Heath, M., Derebail, S. S., Gorelick, R. J. & DeStefano, J. J. (2003). Differing roles of the N- and C-terminal zinc fingers in human immunodeficiency virus nucleocapsid protein-enhanced nucleic acid annealing. *J. Biol. Chem.* **278**, 30755–30763.
22. De Guzman, R. N., Wu, Z. R., Stalling, C. C., Pappalardo, L., Borer, P. N. & Summers, M. F. (1998). Structure of the HIV-1 nucleocapsid protein bound to the SL3 psi-RNA recognition element. *Science*, **279**, 384–388.
23. Bernacchi, S., Stoylov, S. P., Piemont, E., Ficheux, D., Roques, B., Darlix, J. L. & Mely, Y. (2002). HIV-1 nucleocapsid protein activates transient melting of least stable parts of the secondary structure of TAR and its complementary sequence. *J. Mol. Biol.* **317**, 385–399.
24. Krishnamoorthy, G., Roques, B., Darlix, J.-L. & Mely, Y. (2003). DNA condensation by the nucleocapsid protein of HIV-1: a mechanism ensuring DNA protection. *Nucl. Acids Res.* **31**, 5425–5432.
25. Stoylov, S. P., Vuilleumier, C., Stoylova, E., Rocquigny, H. D., Roques, B. P., Gérard, D. & Mély, Y. (1997). Ordered aggregation of ribonucleic acids by the human immunodeficiency virus type 1 nucleocapsid protein. *Biopolymers*, **41**, 301–312.
26. Vuilleumier, C., Bombarda, E., Morellet, N., Gerard, D., Roques, B. P. & Mely, Y. (1999). Nucleic acid sequence discrimination by the HIV-1 nucleocapsid protein NCp7: a fluorescence study. *Biochemistry*, **38**, 16816–16825.
27. Urbaneja, M. A., Kane, B. P., Johnson, D. G., Gorelick, R. J., Henderson, L. E. & Casas-Finet, J. R. (1999). Binding properties of the human immunodeficiency virus type 1 nucleocapsid protein p7 to a model RNA: elucidation of the structural determinants for function. *J. Mol. Biol.* **287**, 59–75.
28. Amarasinghe, G. K., Guzman, R. N. D., Turner, R. B., Chancellor, K. J., Wu, Z. R. & Summers, M. F. (2000). NMR structure of the HIV-1 nucleocapsid protein bound to stem-loop SL2 of the Psi-RNA packaging signal: implications for genome recognition. *J. Mol. Biol.* **301**, 491–511.
29. Cosa, G., Harbron, E. J., Zeng, Y., Liu, H. W., O'Connor, D. B., Eta-Hosokawa, C. *et al.* (2004). Secondary structure and secondary structure dynamics of DNA hairpins complexed with HIV-1 NC protein. *Biophys. J.* **87**, 2759–2767.
30. Azoulay, J., Clamme, J.-P., Darlix, J. L., Roques, B. P. & Mely, Y. (2003). Destabilization of the HIV-1 complementary sequence of TAR by the nucleocapsid protein through activation of conformational fluctuations. *J. Mol. Biol.* **326**, 691–700.
31. Chan, B., Weidemaier, K., Yip, W. T., Barbara, P. F. & Musier-Forsyth, K. (1999). Intra-tRNA distance measurements for nucleocapsid protein-independent tRNA unwinding during priming of HIV reverse transcription. *Proc. Natl Acad. Sci. USA*, **96**, 459–464.
32. Hargittai, M. R. S., Mangla, A. T., Gorelick, R. J. & Musier-Forsyth, K. (2001). HIV-1 nucleocapsid protein zinc finger structures induce tRNA<sup>Lys</sup>3 tertiary structural changes but are not critical for primer/template annealing. *J. Mol. Biol.* **312**, 985–997.
33. Hong, M., Harbron, E., O'Connor, D., Guo, J., Barbara, P. F., Levin, J. G. & Musier-Forsyth, K. (2003). Nucleic acid conformational changes essential for HIV-1 nucleocapsid protein-mediated inhibition of self-priming in minus-strand transfer. *J. Mol. Biol.* **325**, 1–10.
34. Beltz, H., Azoulay, J., Bernacchi, S., Clamme, J. P., Ficheux, D., Roques, B. *et al.* (2003). Impact of the terminal bulges of HIV-1 cTAR DNA on its stability and the destabilizing activity of the nucleocapsid protein NCp7. *J. Mol. Biol.* **328**, 95–108.
35. Williams, M. C. & Rouzina, I. (2002). Force spectroscopy of single DNA and RNA molecules. *Curr. Opin. Struct. Biol.* **12**, 330–336.
36. Williams, M. C., Wenner, J. R., Rouzina, I. & Bloomfield, V. A. (2001). The effect of pH on the overstretching transition of dsDNA: evidence of force-induced DNA melting. *Biophys. J.* **80**, 874–881.
37. Williams, M. C., Wenner, J. R., Rouzina, I. & Bloomfield, V. A. (2001). Entropy and heat capacity of DNA melting from temperature dependence of single molecule stretching. *Biophys. J.* **80**, 1932–1939.
38. Wenner, J. R., Williams, M. C., Rouzina, I. & Bloomfield, V. A. (2002). Salt dependence of the elasticity and overstretching transition of single DNA molecules. *Biophys. J.* **82**, 3160–3169.
39. Williams, M. C., Rouzina, I. & Bloomfield, V. A. (2002). Thermodynamics of DNA interactions from single molecule stretching experiments. *Acc. Chem. Res.* **35**, 159–166.
40. Pant, K., Karpel, R. L., Rouzina, I. & Williams, M. C. (2004). Mechanical measurement of single molecule binding rates: kinetics of DNA helix-destabilization by T4 gene 32 protein. *J. Mol. Biol.* **336**, 851–870.
41. Pant, K., Karpel, R. L. & Williams, M. C. (2003). Kinetic regulation of single DNA molecule denaturation by T4 gene 32 protein structural domains. *J. Mol. Biol.* **327**, 571–578.
42. Pant, K., Karpel, R. L. & Williams, M. C. (2005). Salt-dependent binding of T4 gene 32 protein to single and double-stranded DNA: single molecule force spectroscopy measurements. *J. Mol. Biol.* **349**, 317–330.
43. Krautbauer, R., Fischerländer, S., Allen, S. & Gaub, H. E. (2002). Mechanical fingerprints of DNA drug complexes. *Single Molecules*, **3**, 97–103.
44. Krautbauer, R., Pope, L. H., Schrader, T. E., Allen, S. & Gaub, H. E. (2002). Discriminating small molecule DNA binding modes by single molecule force spectroscopy. *FEBS Letters*, **510**, 154–158.
45. Mihailovic, A., Vladescu, I., McCauley, M., Ly, E., Williams, M. C., Spain, E. M. & Nunez, M. E. (2006). Exploring the interaction of ruthenium(II) polypyridyl complexes with DNA using single-molecule techniques. *Langmuir*, **22**, 4699–4709.
46. Vladescu, I. D., McCauley, M. J., Rouzina, I. & Williams, M. C. (2005). Mapping the phase diagram of single DNA molecule force-induced melting in the presence of ethidium. *Phys. Rev. Letters*, **95**, 158102.
47. Cruceanu, M., Urbaneja, M. A., Hixson, C. V., Johnson, D. G., Datta, S. A., Fivash, M. J. *et al.* (2006). Nucleic acid binding and chaperone properties of HIV-1 Gag and nucleocapsid proteins. *Nucl. Acids Res.* **34**, 593–605.
48. Egele, C., Schaub, E., Ramalanjaona, N., Piemont, E., Ficheux, D., Roques, B. *et al.* (2004). HIV-1 nucleocapsid protein binds to the viral DNA initiation sequences

- and chaperones their kissing interactions. *J. Mol. Biol.* **342**, 453–466.
49. Williams, M. C., Rouzina, I., Wenner, J. R., Gorelick, R. J., Musier-Forsyth, K. & Bloomfield, V. A. (2001). Mechanism for nucleic acid chaperone activity of HIV-1 nucleocapsid protein revealed by single molecule stretching. *Proc. Natl Acad. Sci. USA*, **98**, 6121–6126.
  50. Williams, M. C., Gorelick, R. J. & Musier-Forsyth, K. (2002). Specific zinc finger architecture required for HIV-1 nucleocapsid protein's nucleic acid chaperone function. *Proc. Natl Acad. Sci. USA*, **99**, 8614–8619.
  51. Le Cam, E., Coulaud, D., Delain, E., Petitjean, P., Roques, B. P., Gérard, D. *et al.* (1998). Properties and growth mechanism of the ordered aggregation of a model RNA by the HIV-1 nucleocapsid protein: an electron microscopy investigation. *Biopolymers*, **45**, 217–229.
  52. Martin, S. L., Cruceanu, M., Branciforte, D., Li, P., W.-l., Kwok, S. C., Hodges, R. S. & Williams, M. C. (2005). LINE-1 retrotransposition requires the nucleic acid chaperone activity of the ORF1 protein. *J. Mol. Biol.* **348**, 549–561.
  53. Mely, Y., de Rocquigny, H., Sorinas-Jimeno, M., Keith, G., Roques, B. P., Marquet, R. & Gerard, D. (1995). Binding of the HIV-1 nucleocapsid protein to the primer tRNA(3Lys), *in vitro*, is essentially not specific. *J. Biol. Chem.* **270**, 1650–1656.
  54. Urbaneja, M. A., Wu, M., Casas-Finet, J. R. & Karpel, R. L. (2002). HIV-1 nucleocapsid protein as a nucleic acid chaperone: spectroscopic study of its helix-destabilizing properties, structural binding specificity, and annealing activity. *J. Mol. Biol.* **318**, 749–764.
  55. Fisher, R. J., Rein, A., Fivash, M., Urbaneja, M. A., Casas-Finet, J. R., Medaglia, M. & Henderson, L. E. (1998). Sequence-specific binding of human immunodeficiency virus type 1 nucleocapsid protein to short oligonucleotides. *J. Virol.* **72**, 1902–1909.
  56. Bloomfield, V. A. (1998). DNA condensation by multivalent cations. *Biopolymers*, **44**, 269–282.
  57. Cantor, C. R. & Schimmel, P. R. (1980). *Biophysical Chemistry*, W. H. Freeman and Company, New York.
  58. Frank-Kamenetskii, M. D., Anshelevich, V. V. & Lukashin, A. V. (1987). Polyelectrolyte model of DNA. <Translation> *Soviet Physics - Uspekhi*, **151**, 595–618.
  59. Manning, G. S. (1978). The molecular theory of polyelectrolyte solutions with applications to the electrostatic properties of polynucleotides. *Quart. Rev. Biophys.* **11**, 179–246.
  60. Beltz, H., Piemont, E., Schaub, E., Ficheux, D., Roques, B., Darlix, J. L. & Mely, Y. (2004). Role of the structure of the top half of HIV-1 cTAR DNA on the nucleic acid destabilizing activity of the nucleocapsid protein NCp7. *J. Mol. Biol.* **338**, 711–723.
  61. Chen, Y., Balakrishnan, M., Roques, B. & Bambara, R. A. (2003). Steps of the acceptor invasion mechanism for HIV-1 minus strand strong stop transfer. *J. Biol. Chem.* **278**, 38368–38375.
  62. McCauley, M., Hardwidge, P. R., Maher, L. J., III & Williams, M. C. (2005). Dual binding modes for an HMG domain from human HMGB2 on DNA. *Biophys. J.* **89**, 353–364.
  63. Lee, N., Gorelick, R. J. & Musier-Forsyth, K. (2003). Zinc finger-dependent HIV-1 nucleocapsid protein-TAR RNA interactions. *Nucl. Acids Res.* **31**, 4847–4855.
  64. Smith, S. B., Cui, Y. J. & Bustamante, C. (1996). Overstretching B-DNA: the elastic response of individual double-stranded and single-stranded DNA molecules. *Science*, **271**, 795–799.
  65. Vo, M.-N., Barany, G., Rouzina I., Musier-Forsyth, K. Mechanistic studies of mini-TAR RNA/DNA annealing in the absence and presence of HIV-1 nucleocapsid protein. *J. Mol. Biol.*, in press. doi:10.1016/j.jmb.2006.08.039

Edited by J. Karn

(Received 17 July 2006; received in revised form 8 August 2006; accepted 15 August 2006)  
Available online 30 August 2006